UNCLASSIFIED

(2)

Communications Division

RESEARCH REPORT
ERL-0531-RR

TROPOSPHERIC PROPAGATION MODELLING WITH THE PARABOLIC EQUATION

by

Patricia L. Slingsby

APPROVED FOR PUBLIC RELEASE

UNCLASSIFIED

ELECTRONICS RESEARCH LABORATORY

UNCLASSIFIED

AR-006-452

DSTO AUSTRALIA

ELECTRONICS RESEARCH LABORATORY

Communications Division

RESEARCH REPORT
ERL-0531-RR

TROPOSPHERIC PROPAGATION MODELLING WITH THE PARABOLIC EQUATION

by

Patricia L. Slingsby

SUMMARY

The parabolic equation is a full-wave approximation to the Helmholtz wave equation that, unlike existing ray tracing and coupled mode techniques, readily accommodates two-dimensionally inhomogeneous atmospheres. This report discusses the implementation of a split-step Fourier Transform solution to the parabolic equation and includes examples of coverage diagrams calculated by this method.

Sep ~~OCT~~ 90

COPY No. 40

APPROVED FOR PUBLIC RELEASE

POSTAL ADDRESS: Director, Electronics Research Laboratory, PO Box 1600, Salisbury, South Australia, 5108.

UNCLASSIFIED

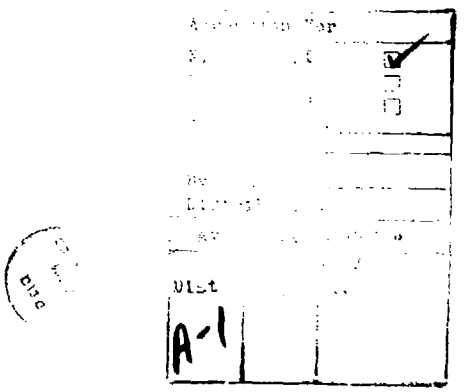

CONTENTS

CONTENTS

FIGURES

GLOSSARY OF METEOROLOGICAL TERMS

Advection	Horizontal movement of an air mass mainly caused by wind movement around high or low pressure systems. Super-refraction due to advection occurs primarily on over-sea paths as an air mass that has become warm and dry over land is carried out to sea where it overlies a layer of cool moist air, establishing both a temperature inversion and an increased humidity lapse rate in the boundary region. The effect can operate in reverse as when cool moist air flows from the sea onto warm dry land.
Coastal Front	Boundary region formed between warm dry air stream above a cool stream caused when air heated over the land surface rises and is replaced by cooler, denser air from the sea so that both a sea breeze near the surface and a strong off-shore movement of dry air is created. Generally extending above 100 km, coastal fronts are common along the western, southern and eastern Australian coasts.
Nocturnal Cooling	Effect common in clear-sky conditions over land paths resulting from a temperature inversion created when air near the ground is cooled considerably whilst the warmer upper air (heated via solar radiation during the day) remains warm. Cloud cover reflects radiation back to the ground, thereby avoiding such cooling. Nocturnal cooling does not occur over sea paths as diurnal ocean temperatures do not vary by much.
Subsidence	Effect due to an air mass which descends and hence is compressed and heated adiabatically. The descending air is very dry since it originated at a high altitude and so an increased humidity lapse and possibly a temperature inversion occurs. Subsidence inversions are more frequent and occur at lower altitudes in winter than in summer.

LIST OF ABBREVIATIONS

CCIR	International Radio Consultative Committee
ERL	Electronics Research Laboratory
FFT	Fast Fourier Transform
IREPS	Integrated Refractive Effects Prediction System
ODE	Ordinary Differential Equation
VHF	Very High Frequency

1 INTRODUCTION

Under the influence of synoptic processes such as advection, subsidence, coastal fronts, or nocturnal cooling, stratification of the troposphere in the form of refractivity layering can occur. If the resulting refraction of propagating electromagnetic waves is sufficiently great to cause a ray curvature that exceeds the curvature of the earth's surface, then the propagating wave can be channelled in a duct. At VHF and higher frequencies, surface and elevated tropospheric ducts can cause extended propagation well beyond the radio horizon with little attenuation relative to free space. The received radio signals can then be markedly stronger (or weaker) than would be expected for a standard atmosphere. The anomalous propagation of energy via a duct can thereby lead to the volatile problem of inter-system interference, whilst radar detection ranges can be enhanced for targets located within the duct. However, ducts can also decrease radio (radar) operational ranges by causing "holes" in signal coverage if a receiver (target) is located outside the duct. Reliable prediction of such anomalous propagation effects can therefore enhance the effective deployment of communications, surveillance and electronic warfare systems.

Propagation prediction models tend to fall into two categories: those methods based on optical ray tracing techniques; and those relying on mode theory. Although qualitative predictions can be made using ray theory, problems associated with the focusing of rays and identification of ray families render these methods unsuitable for modelling diffraction effects in non-standard atmospheres. Mode theory, which involves a full-wave solution to Maxwell's equations, can be applied to ducting problems but becomes intractable when complex refractive structures are involved. Computing cost tends to limit convergent solutions for modal analysis to simple refractive structures. Neither of these methods, nor existing hybrid combinations of these, can be readily applied to the two-dimensionally inhomogeneous atmospheres of range-dependent problems.

Since the wave equations governing realistic physical representation of the troposphere permit a closed form solution only in very simple cases, approximations to these equations have been introduced that, with the availability of modern numerical techniques and fast computers, facilitate solution of complicated propagation problems. This report demonstrates the application of an alternative full-wave model that is based upon such an approximation to the wave equation and can be applied to complicated range-dependent tropospheric propagation problems. The parabolic equation was first obtained for propagation over a spherical earth in a vertically inhomogeneous, horizontally homogeneous atmosphere by (Leontovich and Fock, 1946) and has been extended by (Ko *et al*, 1984) for the case of a two-dimensionally inhomogeneous atmosphere to give a parabolic partial differential equation for the field amplitude. The model presented in this report uses a split step Fourier transform technique which takes advantage of the computational speed of the Fast

Fourier Transform algorithm and is numerically stable. This solution method was developed in the underwater acoustics arena by (Hardin and Tappert, 1973) to solve a parabolic equation of identical form to the parabolic equation for tropospheric propagation. The use of this technique affords a full-wave solution without the large computational overheads of previous full-wave methods. It is this property of the method which makes it most attractive.

This report begins with a brief description of the wave equation governing two-dimensional tropospheric propagation and indicates how propagation problems can be represented by a partial differential equation with complex coefficients. After a discussion of the applicability of existing prediction techniques for ducting environments, it is shown how the tropospheric wave equation reduces to a parabolic equation that facilitates ready solution. This approximation to the wave equation has the significant advantage that it invites "marching" type solutions since the partial differential equation is now only first order in range.

The third section, "Split step Fourier Solution", is devoted to a description of the solution method chosen to evaluate the parabolic equation of section 2. The split step solution is a "marching" type solution since the solution can be evaluated at range $x+\delta x$ (δx is sufficiently small) by using the evaluated solution at range x as an initial value for calculations. Providing that appropriate boundary conditions are satisfied the solution can in this way be stepped out to the required range. The entire range- and height-dependent field is calculated as the solution is marched forward in this manner. The solution involves the discretisation of the electromagnetic field with respect to height at each range step and the use of the Fast Fourier Transform. In this section, solution stability is considered and an indication of the errors inherent in the technique is also given.

Since a marching solution can be applied to the parabolic equation, a maximum range boundary condition need not be specified, thus simplifying computation. Tropospheric propagation problems can therefore be specified as initial boundary value problems on an open domain. Section 4 deals with the specification of this initial starting field and of the surface and maximum altitude boundary conditions. There are however some signal processing aspects of implementation that need to be addressed, and included in this section is a discussion of these. The following section contains an analysis of solution sensitivity to perturbations in initial field and to small-scale discontinuities in refractive index profiles.

Within a simplified ray tracing context, section 6 illustrates the effects that variations in refractive structures have upon tropospheric propagation. The main purpose of this section is to introduce the categories of ducting profiles that are modelled in section 7.

The report concludes with representative examples of coverage diagrams generated using the split step solution to the parabolic wave equation. These diagrams are instructive as examples which illustrate the complicated nature of coverage patterns resulting from common refractive index structures. They were generated on a COMPAQ 386/20e personal computer with an Eighteen Eight Labs fast parallel processing board. The program used to generate the diagrams in this report is currently under development in Communications Division, Electronics Research Laboratory (ERL) at Defence Science and Technology Organisation. It accepts environmental data for the propagation paths of interest in the form of refractivity profiles (specified either analytically or by measurement data) and generates two-dimensional Height-Range coloured intensity plots for the area of maximum height and range specified by the operator. The program has also been used to generate two-way path loss diagrams for radar applications (Slingsby, 1990).

In addition to the large computational saving over other full-wave methods, a major advantage of the parabolic equation technique outlined in this report is that it affords progressive calculation of the propagated field from one range location to the next. Hence the ERL developmental software has potential application as an interactive research tool by which an operator would be able to create desired propagation patterns through interactive manipulation of the input environmental parameters. This is an advantage which other applicable techniques that have been developed to date do not have. For those, the environmental input information needs to be defined before computation commences. Thus given a means of remotely sensing the atmospheric refractivity data, the ERL developmental software could be adapted to provide a real-time updating display illustrating the effects of the transient weather conditions on signal propagation.

2 TROPOSPHERIC WAVE PROPAGATION PROBLEMS

This section formulates the tropospheric wave propagation problem and, after a brief discussion of prediction techniques currently available for modelling ducting effects, introduces the parabolic approximation to the elliptic wave equation. Consideration of the significance of this approximation for tropospheric propagation problems indicates that for realistic ducting environments the assumptions inherent in this parabolic approximation are valid. Whereas in usual numerical schemes the elliptic wave equation requires solution of a large system of simultaneous equations in a large number of unknowns with boundary conditions being specified on a closed domain, the parabolic equation can instead be solved by a 'marching' technique on an open domain; so numerical solution is easier to compute.

2.1 Governing wave equation

The Helmholtz wave equation for the electric or magnetic field, Φ, of an isotropic time-harmonic point source is given by

$$\nabla^2 \Phi + k^2 n^2 \Phi = 0 \qquad (1)$$

where ∇^2 is the Laplacian operator, $k=2\pi/\lambda$ is the free space wavenumber and $n=\sqrt{(\epsilon - j\sigma)/w\epsilon_0}$ is the index of refraction, with ϵ_0 denoting free space permittivity and ϵ, σ representing the absolute permittivity and conductivity respectively of the propagating medium.

In order to examine the spherical spreading behaviour from a point source of electromagnetic waves along a spherical earth it is convenient to adopt the spherical coordinate system (r,θ,ϕ) with the origin at the centre of the earth and with the polar axis drawn through the source ($\theta=0$ at the source). The first assumption to be made in this study is that of azimuthal symmetry. This is introduced for two reasons: firstly, it is rare that sufficient environmental information is available to warrant the computational overhead for a full three-dimensional solution to the wave equation; and secondly, it is assumed that the azimuthal variations of refractive index will be sufficiently slow to justify a two-dimensional approach. The field, Φ, and refractive index, n, will in this case be functions of (r,θ) only. The tropospheric wave propagation problem can therefore be viewed in terms of a closed-domain boundary value problem, as indicated by figure 1.

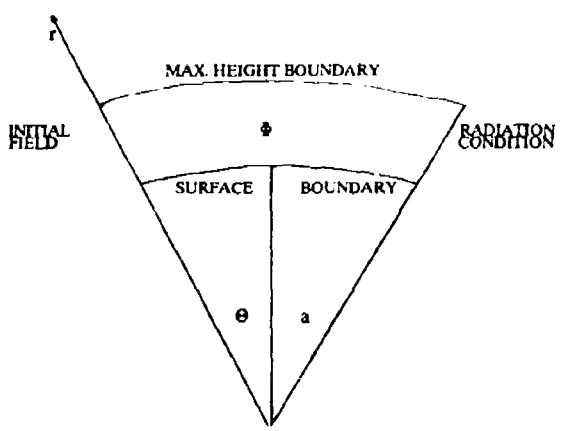

Figure 1 Tropospheric boundary value problem

The assumption of azimuthal symmetry means that $(\partial/\partial\phi) \equiv 0$ in Maxwell's equations. For an electric dipole, then, only field components E_r, E_θ and H_ϕ will be non-zero; and for a magnetic dipole, only H_r, H_θ and E_ϕ will exist. In the case of an electric dipole, Maxwell's equations reduce to :-

$$\frac{1}{r}\left[\frac{\partial}{\partial r}(rE_\theta) - \frac{\partial E_r}{\partial \theta}\right] + j\omega\mu_0 H_\phi = 0$$

$$\frac{1}{r\sin\theta}\left[\frac{\partial}{\partial\theta}(H_\phi \sin\theta)\right] = j\omega\epsilon E_r$$

$$-\frac{1}{r}\frac{\partial}{\partial r}(rH_\phi) = j\omega\epsilon E_\theta$$

and combining these three equations to eliminate field components E_r and E_θ

$$\frac{1}{r}\left\{\frac{\partial}{\partial r}\left[-\frac{1}{\epsilon}\frac{\partial}{\partial r}(rH_\phi)\right] - \frac{1}{r}\frac{\partial}{\partial\theta}\left[\frac{1}{\epsilon\sin\theta}\frac{\partial}{\partial\theta}(H_\phi\sin\theta)\right]\right\} - \omega^2\mu_0 H_\phi = 0 \qquad (2)$$

Expanding (2), using the subscripts r and θ to denote $\frac{\partial}{\partial r}$ and $\frac{\partial}{\partial\theta}$ respectively, and dropping the ϕ subscript from the scalar H_ϕ:

$$H_{rr} + \frac{2H_r}{r} - \frac{H}{r^2} - \frac{H\cot\theta}{r^2} + \frac{H_\theta\cot\theta}{r^2} - \frac{H_r\epsilon_r}{\epsilon} - \frac{H\epsilon_r}{r\epsilon} - \frac{H\cot\theta\,\epsilon_\theta}{r^2\epsilon} + \frac{H_{\theta\theta}}{r^2} - \frac{H_\theta\epsilon_\theta}{r^2\epsilon} + k^2n^2H = 0 \qquad (3)$$

since

$$\epsilon = \epsilon_0 n^2$$

and

$$\omega^2\mu_0\epsilon_0 = k^2$$

Equation (3) can be represented in the form

$$\nabla^2\bar{H}_\phi + k^2n^2\bar{H}_\phi + \frac{\nabla\bar{\epsilon}}{\epsilon} \times (\nabla \times \bar{H}_\phi) = 0 \qquad (4)$$

2.2 Existing prediction techniques

There exists a large body of literature devoted to the theory of ray tracing and coupled mode techniques, and so these will receive only a cursory treatment here. Hybrid combinations of ray tracing and mode methods also exist; perhaps the most widely used of these is the Integrated Refractive Effects Prediction System (IREPS) developed by the Naval Ocean Systems Centre, San Diego. However, IREPS does not overcome many of the limitations inherent in ray tracing and mode methods used for ducting applications.

The main purpose of this section is to highlight the deficiencies of such techniques thereby emphasising the advantage to be gained through implementation of the alternative parabolic equation method.

2.2.1 Geometrical optics

The general geometrical theory can be found in a number of works. See, for example, (Budden, 1961).

Assuming that the refractive index of the medium is slowly varying in space, then an approximate solution to the wave equation (1) is sought in the form

$$\Phi(r) = A(r)\, e^{-jkS(r)} \tag{5}$$

where A(r) and S(r) are slowly varying functions of position vector r; the function S, known as the iconal function, defines surfaces of constant phase. For this solution to satisfy the reduced wave equation it is necessary that

$$|\nabla S|^2 = n^2(r) \tag{6}$$

and

$$A(r)\,\nabla^2 S(r) + 2\,\nabla S(r)\,A(r) = 0 \tag{7}$$

hold. The surfaces S(r) = constant are the wave fronts and so the ray paths along which the electromagnetic waves propagate are given by the trajectories orthogonal to these surfaces (ie $|\nabla S|^2$). Integration of equation 6 (known as the iconal equation) and of equation 7 give ray trajectories and wave amplitude.

If the atmospheric refractive index can be assumed to be spherically stratified with respect to the surface of the earth (it is horizontally homogeneous, varying with altitude only), then equation (6) is equivalent to Snell's law and

$$n(h)\sin\Theta = S \tag{8}$$

where Θ is the angle that a ray makes with the vertical, S is a constant for each ray, and h refers to altitude measured from the earth's surface. The radius of curvature of a ray, ρ, is then given by (Livingston, 1970)

$$\rho = \frac{-n}{\frac{dn}{dh}\sin\Theta} \tag{9}$$

There are several limitations to ray tracing techniques. The first of these relates to an assumption that the fractional change in spacing between neighbouring rays (initially parallel) is small with respect to a wavelength. In a ducting environment, where rays are 'trapped' and are strongly refracted or reflected, this requirement will be violated.

Another limitation of ray tracing techniques involves the identification of ray families. A ray is assumed to be a typical member of a "family" that consists of a set of rays with similar initial conditions and which have followed similar paths. In order to calculate the field at a given point, the contribution of each ray passing through that point must be determined, and therefore the ray families must be identified. Errors occur when rays are incorrectly identified, in which case their contribution to the total field will be inaccurately calculated.

At caustics (surfaces occurring where adjacent rays from the same family intersect), the above ray equations will have multiple solutions; and at extended ranges, as more caustics are generated, ray theory tends to break down completely. Asymptotic approximations for the vicinity of caustics tend to be complex and to date no simple method has been developed that would encourage ready implementation of such approximations.

Frequency does not enter into ray tracing treatments of propagation in ducting environments and so errors are introduced due to the dependence on frequency in determining whether a ray will be trapped by a given duct structure. In addition, it is a requirement of ray theory that the path-length difference between direct and reflected rays be at least one-quarter wavelength (Fishback, 1951). Ray theory methods are therefore limited to regions within the radio horizon.

Ray tracing methods follow very simple geometry and yield a convenient qualitative picture of ducting phenomena. However the tendency of ray theory to reflect all or nothing of the rays from ducting layers is another limitation of these techniques, as appreciable ducting is only indicated when both transmitting and receiving antennas are within the duct. By ray theory, a wave originating exterior to a duct generally cannot be trapped within the duct, and there is no allowance for leakage from the duct by trapped waves. Partial reflection from ducting layers has not yet been adequately addressed. Similarly, lateral changes in refractive index have been considered by a small number of authors although results have been of a qualitative, rather than quantitative nature.

2.2.2 Coupled Mode Techniques

Since ray tracing theory does not accommodate non-standard atmospheres well, in dealing with ducting environments a full-wave solution to Maxwell's equations is often sought. The waveguide model for electromagnetic propagation in a tropospheric duct treats such propagation as being analogous to propagation in a leaky waveguide. For

comprehensive treatment of such methods refer to (Booker and Walkinshaw, 1946), (Kerr, 1951) and (Budden, 1961).

In the tropospheric wave problem, as formulated in section 2.1, the surface of the earth acts as a curved boundary from which electromagnetic waves may be reflected and around which these waves may be diffracted. If the refractive index, n(h), is assumed to be spherically stratified with respect to the surface of a smooth earth, then in terms of an earth flattened geometry, earth curvature is included in a modified index of refraction as defined by

$$m(h) = n(h) + \frac{h}{a} \tag{10}$$

where h denotes altitude measured from the earth's surface, and a is the radius of the earth. The field of a source in a stratified atmosphere can then be represented by a sum of leaky waveguide modes. For a dipole source, the field will be proportional to

$$\frac{1}{\sqrt{R}} \sum_{S=S_n} e^{-ikSR} F_t(h) F_r(h) e \tag{11}$$

(Budden, 1961)

where R is the horizontal range, k is the free space wavenumber, e represents the excitation of the mode, and $F_t(h)$, $F_r(h)$ determine the attenuation of the mode with height (normalised to unity at the earth's surface) for transmitter and receiver respectively. The terms F(h) can be expressed in terms of the height-gain function g(h,S): $F(h) = g(h,S)/g(0,S)$; where g(h,S) is the outgoing wave solution of

$$\frac{d^2 g(h,S)}{dh^2} + k^2 [m^2(h) - S^2] g(h,S) = 0 \tag{12}$$

Since S is complex, the term $\exp^{-ikSR}$ in equation (11) determines the attenuation of the mode with range.

In order to determine the allowed modes it is necessary to apply boundary conditions. Firstly, the radiation boundary condition requires that waves are only outgoing. If the changes in refractivity gradient associated with ducting layers are represented in a vertical modified refractive index profile by discontinuities in a linear segmented profile, then this radiation condition puts a constraint on the height-gain function at heights above the discontinuity of a ducting layer. Secondly, the boundary condition at the earth's surface must be satisfied. This constrains the height-gain function in the region below a ducting layer. Finally, the height-gain functions and their derivatives

above and below the discontinuities at the boundaries of a ducting layer, are required to be continuous across those discontinuities. This last boundary condition leads to the mode equation, the details of which can be found in most papers dealing with coupled mode theory. The reader is referred to (Craig, 1985) for a useful interpretation of the roots of the mode equation in terms of the familiar ray theory picture.

Locating the roots of the modal equation is a complex task and much research has been channelled towards this. Various numerical solution techniques have been investigated in respect to this problem but these will not be discussed here. The reader is referred to (Rotheram, 1983) for a survey of existing solution methods.

Perhaps the most significant disadvantage associated with modal techniques is the complexity of solutions. The number of modes which need to be considered for ducting problems is proportional to frequency and to the thickness of the duct. Modal methods can therefore become intractable at high frequencies and when complicated duct profiles are involved.

Experimental verification of waveguide models has been largely qualitative. Undoubtedly this reflects the difficulty of adequately monitoring refractivity structures during experimental studies, but it also indicates some inadequacy of the modal ducting model. Observational data indicate received fields appreciably stronger than can be accounted for by the simple homogeneous duct structures considered in most mode analyses. A number of authors (see, for example, Barton, 1973) have suggested the presence of ducting layers that vary with range as a cause of such observed phenomena. Although there have been some attempts to address problems involving refractive structures which vary with range as well as with height (refer to Wait, 1980, for example), the results have again been qualitative in nature. Computation is also considerably increased in such approaches over that for the homogeneous ducting problems. Thus most implementations restrict the refractive index to be a simple analytical function of height alone, and therefore have application only to range-independent problems. The most common problem of this type involves low-level evaporation ducts over the ocean. For problems involving surface and elevated ducts, however, modal models tend not to be applicable.

2.2.3 IREPS

The Integrated Refractive Effects Prediction System (Hitney and Richter, 1976) has been used since 1978 by the United States Navy and other organisations to give an

operational propagation assessment capability for naval surveillance, communications, electronic warfare and weapon guidance systems. It is designed to deal with evaporative and surface-based ducting, and so does not model well the propagation effects of elevated ducts.

The products IREPS produces are based upon a combination of ray-optics and a simplified full-wave single-mode solution, with semi-empirical formulations based on measured data and interpolations to smooth transitions between the various models. Polarisation effects are neglected by IREPS on over-the-horizon paths which, like the methods discussed in sections 2.2.1 and 2.2.2, assumes range-independence of the ducting structures. An example of a coverage diagram generated by IREPS is included at figure 2, where the signal coverage for a homogeneous duct between 50 m and 600 m has been modelled. (The duct modelled here is of identical strength and extent to that used for figure 8, page 31, in which the parabolic equation method was employed to generate signal coverage from a gaussian beam antenna.)

For airborne applications particularly, elevated ducts assume a greater significance in the prediction of propagated signals. For these ducts it is no longer adequate to assume horizontal homogeneity of the inversion layers. Real-time modal calculations are prohibitive due to the computational intensity involved in such analysis; whilst the approach adopted by IREPS of "template matching" - whereby precalculated results are scaled to the frequency and duct height of interest - would be very difficult to extend for the case of elevated ducting layers (since the single-mode approximation currently used for beyond-the-horizon ranges would no longer be valid for these elevated ducts, for which multi-mode propagation is important). For such reasons, the approach of the parabolic equation and split-step Fourier solution becomes very attractive.

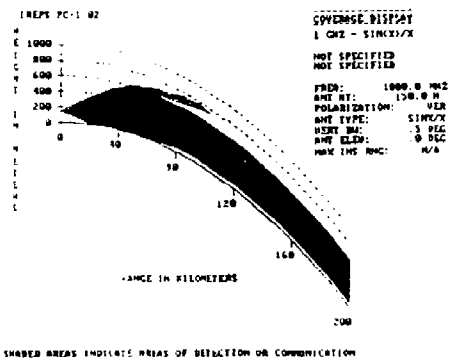

Figure 2 IREPS coverage diagram for 600 m homogeneous duct

2.3 Parabolic Equation

By making the substitution

$$H_\phi(r,\theta) = \frac{u(r,\theta)\, e^{ika\theta}}{r\,\epsilon(r,\theta)\sqrt{\sin\theta}} \tag{13}$$

as suggested by (Ko *et al*, 1984), equation (3) becomes

$$u_{rr} - u_r\left(\frac{3\epsilon_\theta}{\epsilon} + \frac{\epsilon_{rr}}{\epsilon}\right) + u_\theta\left(\frac{2ka}{r^2} - \frac{3\epsilon_\theta}{r^2\epsilon} + \frac{\cot\theta}{r^2}\right) + \frac{u_{\theta\theta}}{r^2} + u\left(3\left(\frac{\epsilon_r}{\epsilon}\right)^2 - \frac{3}{2r^2} - \frac{9\cot^2\theta}{4r^2}\right.$$
$$\left. + \frac{ika\cot\theta}{r^2} - \frac{3\cot\theta\,\epsilon_\theta}{2r^2\epsilon} - \frac{k^2a^2}{r^2} - \frac{3ika\epsilon_\theta}{r^2\epsilon} - \frac{\epsilon_{rr}}{r^2\epsilon} + \frac{3}{r^2}\left(\frac{\epsilon_\theta}{\epsilon}\right)^2 - \frac{3\cot^2\theta}{4r^2} + k^2n^2\right) = 0 \tag{14}$$

The effect of the substitution of equation (12) is to remove the rapid phase variation of the field H_ϕ. The $k^2\,(n^2 - 1)$ term in (13) arises from the approximation $k^2 a^2 / r^2 \approx k^2$ since, in the troposphere, altitude above the earth will be small compared to the radius of the earth, a. Equation (14) can then be reduced to

$$u_{zz} + 2iku_x + k^2\left(n^2 - 1 + \frac{2z}{a}\right)u = 0 \tag{15}$$

when the following approximations are assumed:-

$$ka u_\theta \gg u_{\theta\theta} \qquad \text{(a)} \qquad\qquad \theta > \frac{100}{ka} \qquad \text{(c)}$$

$$\frac{\epsilon}{\epsilon}\theta \le \frac{ka}{100} \qquad \text{(b)} \qquad\qquad \frac{\epsilon}{\epsilon_r} \gg \left(\frac{2k^2}{a}\right)^3 \qquad \text{(d)}$$

and the following earth-flattening substitutions are incorporated:-

$$z = r - a \tag{16}$$

$$x \approx a\theta \tag{17}$$

$$n(x,z) = n(r,\theta) + \frac{2z}{a} \tag{18}$$

Equation (15) is known as the parabolic equation since it is second-order in altitude, z, and first-order in range, x. The advantage that an equation of this form has over that of equation (3) is that solution to the parabolic equation does not require that the maximum range boundary be specified. Subsequently, the parabolic equation invites a "marching" solution in which the equation is solved at initial range x=0 and is then solved for small steps out in range, using the solution at the previous step as the starting field for the present calculation. In this way the solution can be calculated out to any range, providing that initial field, upper and surface boundary conditions are satisfied. Such a solution is inherently easier to compute than one which requires a large number of unknowns with boundary conditions being specified on a closed domain, as is the case for the full elliptic wave equation. The tropospheric wave

propagation problem can now be considered in terms of the open-domain boundary value problem of figure 3.

The resulting model is conceptually simple, as it applies equally well at short and long ranges (in the far field), unlike either ray tracing or modal models. Like ray tracing and coupled mode analysis, however, the parabolic equation neglects the backscattered field. This can be seen with reference to equation (12) in which only the positive exponential term $e^{ikx\theta}$ is included. Other restrictions inherent in the parabolic approximation are discussed below.

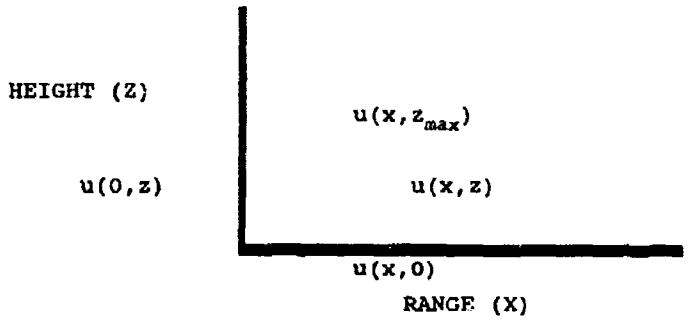

Figure 3 Parabolic equation boundary value problem

2.3.1 Assumptions

The effect of the paraxial approximation can be seen by substituting a trial plane wave solution into the two-dimensional wave equation (3,14) and into the parabolic equation (15) and then comparing the results. If the wavenumber components in the x- and z-directions are denoted are denoted by k_x and k_z respectively, then a plane wave solution to equation (14) can be expressed by

$$u = \exp[i (k_x x + k_z z)]$$

Substituting this into equation (14) gives

$$-k_z^2 u + 2ik_x ku - k_x^2 u + k^2 (m^2 - 1) = 0$$

that is,

$$k_x = \pm \sqrt{k^2 (1+m^2 -1) - k_z^2}$$

Now $m^2 \approx 1$ so that

$$k_x = \pm \sqrt{k^2 - k_z^2}$$

If Θ now specifies the angle of propagation with respect to horizontal, then this equation is merely a statement of the trigonometric identity

$$\cos\Theta = \pm \sqrt{1 - \sin^2\Theta}$$

The plane wave solution to the parabolic equation (equation 15) can be expressed in the form

$$u = \exp[i\{(k_x - k)x + k_z z\}]$$

Substituting into equation (14) gives

$$-k_z^2 - 2(k_x - k)k + k^2(m^2 - 1) = 0$$

which can be reexpressed as

$$-k_z^2 - 2k_x k + k^2(2 + m^2 - 1) = 0$$

Now $m^2 \approx 1$ so

$$k_x = k - \frac{k_z^2}{2k}$$

which corresponds to

$$\cos\Theta = 1 - \frac{\sin^2\Theta}{2}$$

This is a good approximation provided that Θ is less than 15-20°. This limitation on the maximum angle of propagation is acceptable for ducting problems since it is only the energy at small angles to the horizontal (typically smaller than 1 degree) that will be trapped by the duct. Therefore energy at angles greater than a few degrees from horizontal need not be considered, thereby allowing a saving in computation (refer to section 4.3 for details).

The second assumption (b) can be rewritten in rectangular coordinates:

$$\frac{\epsilon}{\epsilon_x} \leq \frac{k}{100} \qquad (19)$$

The term ϵ / ϵ_x can be associated with the radius of curvature of propagated energy rays resulting from horizontal variations in ϵ. Equation (19) can then be represented in the form $\epsilon / \epsilon_x \geq 100\lambda/2\pi$, implying that the radius of curvature of propagating rays must be large with respect to a wavelength. In other words, equation (19) infers

that horizontal variation in ϵ must be reasonably slow. Since $\epsilon = \epsilon_0 n^2$, $\epsilon / \epsilon_x = n^2 / n^2_x$, which can be approximated by $n^2 \delta x / \delta n^2$. So for a worst-case frequency of 30 MHz[1] and for a typical value of n (say 1.00035), δn^2 must be smaller than, or equal to, 0.00629/m, which, in practice, will be satisfied. Thus assumption (b) is valid for the frequency ranges over which this method is applicable. Similarly, assumption (d) implies that vertical variations in refractive index must be slow.

Assumption (c), rewritten in rectangular coordinates, becomes

$$x > \frac{100}{2\pi}\lambda \tag{20}$$

This implies that the parabolic equation neglects the near-field effects, since equation (20) is only valid at ranges greater than sixteen wavelengths from the source.

Like ray tracing and coupled mode theory methods, the parabolic equation neglects the backscattered field. It does however retain all diffraction effects associated with the propagating medium and is therefore valid in regions where problems with focusing of rays and identification of ray families cause ray tracing methods to break down. The parabolic equation also retains the full coupling between waveguide modes that mode theory requires for horizontally inhomogeneous atmospheres.

3 SPLIT STEP FOURIER SOLUTION

To model problems of tropospheric propagation in ducting environments, a solution to equation (14) is required for realistic range-dependent refractive index structures. The most tractable algorithm that has been developed to date, and the one which is the easiest to implement, is the split step Fourier solution developed in the underwater acoustics arena by (Hardin and Tappert, 1973), which uses the computational speed of the Fast Fourier Transform to advance solution over one range step size, δx.

3.1 Formulation

Equation (15) can be re-expressed in the form

$$u_x(x,z) = \left[i \frac{k}{2} \{ n^2(x,z) - 1 \} + \frac{1}{2k} \frac{\partial^2}{\partial z^2} \right] u(x,z)$$

$$= i \left[A(x,z) + B(z) \right] u(x,z) \tag{21}$$

1. At frequencies below VHF, ionospheric effects become increasingly important.

where

$$A(x,z) = \frac{k}{2}\{m^2(x,z) - 1\}$$

and

$$B(z) = \frac{1}{2k}\frac{\partial^2}{\partial z^2}$$

If the index of refraction can be assumed to be slowly varying with range, then the solution of (21) will then take the form

$$u(x+\delta x, z) = i\,\delta x \exp(A+B)\,u \tag{22}$$

provided that the commutator

$$\left[\ (A+B),\ \int (A+B)\,dx\ \right] = 0$$

In general, this will only be true if A(x,z) is independent of altitude, z - a restriction which would render this solution useless for problems involving ducting structures. Instead, this condition restricts the application of such a solution to environments in which A is sufficiently slowly varying with respect to altitude that the error incurred by this assumption is negligible.

The split step Fourier algorithm involves the assumption that

$$u(x+\delta x, z) = e^{iA\delta x}\, e^{iB\delta x}\, u(x,z) \tag{23}$$

The validity of this assumption requires that

$$[\,A, B\,] = 0$$

where [A,B] = AB-BA denotes the commutator of A and B. Again this does not hold, since

$$e^{A+B} = e^{A}\ e^{B}\ e^{C_2}\ e^{C_3} e^{C_4} \ldots$$

where C_k is a linear combination of k-fold commutators of A and B. In particular,

$$C_2 = -\frac{1}{2}[A,B];\ C_3 = \frac{1}{6}[A,[A,B]] + \frac{1}{3}[B,[A,B]]$$

(For discussion of this exponential identity, refer for example, to Steinberg, 1985.)

The evaluation of $\exp^{iA\delta x}$ is straight-forward. Since B(z) contains a second-order differential operator in z, the term $e^{iB\delta x}u(x,z)$ can be evaluated by means of a Fourier transform operation between the spatial domain, z, and the spatial frequency variable p ($p = k \sin\Theta$,

where Θ represents the angle of propagation from the horizon):

$$e^{iB\delta x}u(x,z) = f^{-1}\{ f[e^{iB\delta x}u(x,z)] \}$$

where

$$f\{u(x,z)\} = \sqrt{\frac{1}{2\pi}}\int_{-\infty}^{+\infty} u(x,z)\, e^{-ipz}\, dz$$

$$f^{-1}\{u(x,z)\} = \sqrt{\frac{1}{2\pi}}\int_{-\infty}^{+\infty} u(x,z)\, e^{-ipz}\, dz$$

So equation (23) becomes

$$\begin{aligned} u(x+\delta x, z) &= e^{iA\delta x} f^{-1}\{ f[e^{iB\delta x}u(x,z)] \} \\ &= e^{ik\delta x(n^2-1+2z/a)/2} f^{-1}\{ e^{-ip\delta x/2} f[u(x,z)] \} \end{aligned} \qquad (24)$$

Equation (24) is obviously an iterative solution, where the field at any range can be evaluated by advancing the solution in small steps, given an initial field u(0,z) and satisfaction of the boundary conditions at the earth's surface and at some maximum altitude. The solution at each range is advanced in two stages: firstly, the field is advanced as if the propagation medium was homogeneous, thus accounting for diffraction effects alone (this is the contribution of the forward and inverse Fourier transform operations of equation (24)); and secondly, the effects of the meteorological environment are applied to the field (the n^2 in the first exponential term of equation (24) accounts for these). The vertical refractive index profiles required for this term are usually obtained from radiosonde data, or they can be modelled analytically. Since equation (24) is a marching solution, different refractive index profiles can be entered into the calculations at each range step, thereby facilitating simple treatment of inhomogeneous atmospheres. It is important to note that, with this solution method, complicated refractive structures (varying in both vertical and horizontal directions) do not require any additional computation to that for standard atmospheres. It will be recalled that for the other full-wave methods discussed in section 2.2.2, the computational overhead of the solutions is proportional to the number of modes required to model the relevant refractive structures.

The error involved in the assumption of equation (24) can be obtained by differentiating (23) and comparing with (21). To third order terms, the error is

$$\delta x[ikm\frac{\partial m}{\partial x}u + m\frac{\partial m}{\partial z}\frac{\partial u}{\partial z} + \frac{mu\partial^2 m}{2\partial z^2} + \frac{u}{2}(\frac{\partial m}{\partial z})^2] - (\partial x)^2\,\frac{iku}{2}(m\frac{\partial m}{\partial z})^2 + O[(\partial x)^3] \quad (25)$$

However, this error is dependent on the particular "split" chosen for the exponential terms in A and B. The regime chosen by (Hardin and Tappert, 1973), for example, assumes

$$u(x+\delta x) \approx e^{i\delta xB/2}\, e^{i\delta xA}\, e^{i\delta xB/2}\, u(x,z)$$

The error incurred by assuming the operators A and B commute in this way is

$$\frac{(\partial x)^3}{96}\{k(\frac{\partial m^2}{\partial z})^2\, u - \frac{4}{k}\frac{\partial^2 m^2}{\partial z^2}\frac{\partial^2 u}{\partial z^2} - \frac{4}{k}\frac{\partial^3 m^2}{\partial z^3}\frac{\partial u}{\partial z} - \frac{1}{k}\frac{\partial^4 m^2}{\partial z^4}\} + \ldots$$

The optimal splitting that will minimise solution error is thus a subject for further research.

3.2 Stability

In this section the requirement of solution stability is investigated. A solution perturbation analysis is included in section 5.

The solution formulated in section 3.1 will be stable if the difference between the theoretical and numerical solutions remains bounded as the solution is stepped out in range. From equation (25) it is evident that the error will be bounded as long as the refractive index gradients remain bounded. In other words, as long as the refractive index gradients are such as to accommodate the requirements of the assumptions discussed in section 2.3.1, the solution will be stable.

4 ASPECTS OF IMPLEMENTATION

This section deals with implementation of the solution of section 3. To date, this solution appears to be the most computationally efficient method that can be applied to modelling tropospheric propagation in ducting conditions. However other solutions have been developed for underwater acoustics applications. The underwater acoustics problem is very similar to the tropospheric case but includes the complication of a sea-bottom boundary condition. (Kewley *et al*, 1984) found that the interaction of this boundary in shallow water problems rendered the split step Fourier solution unsuitable for modelling underwater problems of this type. Several alternative solutions have been developed. For example, whereas in the split step Fourier scheme the second order partial differential operator in height of the parabolic equation is represented by the inverse Fourier transform of its Fourier transform, in the ordinary differential equation (ODE) approach adopted by (Lee and Papadakis, 1980), this operator is approximated by a central finite difference operator which converts the partial differential equation into a system of first order ODEs which are then solved by application of a nonlinear multistep numerical method. Another solution, proposed by (Lee, Botseas and Papadakis, 1981), uses the Crank-Nicolson scheme for variable coefficients to solve the parabolic equation. These alternate solutions may prove useful for complicated tropospheric problems, but the increased computational intensity involved with these, when compared with that of the split step Fourier solution, is a major disincentive.

The following is a discussion of the application of initial and boundary conditions to the split step solution of section 3, and begins with a description of the way in which the surface boundary condition is incorporated into the present implementation. The specification of the maximum height boundary is included in section 4.3, "Signal Processing Aspects", as the particular implementation of this condition is a consequence of application of the discrete Fourier transform. At this maximum height boundary a pseudo radiation condition is introduced by smooth attenuation of the field. Other aspects of implementation that are introduced as a by-product of the discrete Fourier transform are also included under section 4.3.

4.1 Surface boundary condition

With the assumption that the skin depth of electromagnetic radiation within the earth is small compared to the earth's radius of curvature, the boundary condition at the surface of a smooth, finitely conducting earth can be approximated by (Senior, 1960):

$$\frac{d}{dz}\, u(x,0) + ik\eta\, u(x,0) = 0 \tag{26}$$

where

$$\eta_V = \sqrt{\mu_r / \left(\epsilon_r + \frac{i\sigma}{\omega\epsilon_0}\right)} \tag{27}$$

$$\eta_H = \sqrt{\left(\epsilon_r + \frac{i\sigma}{\omega\epsilon_0}\right) / \mu_r} \tag{28}$$

can be substituted into (26) for vertical and horizontal polarisation respectively. In these expressions ϵ_r and σ are the relative permittivity and absolute conductivity of the surface medium respectively, and ϵ_0 is the free space permittivity. ω is the radian frequency of the propagating electromagnetic waves, while μ_r refers to the relative permeability of the surface medium, which is often assumed to be unity.

Polarisation of the propagating waves is incorporated in the surface boundary condition. From (27) and (28) it is evident that for a perfectly conducting surface $\frac{\partial}{\partial z}u(x,0)=0$ (vertical polarisation) or $u(x,0)=0$ (horizontal polarisation), in which case the field must be symmetric or antisymmetric respectively about the surface. The surface boundary condition can therefore be satisfied using a linear combination of even and odd solutions at each step, with the assumption that their complex combination ratio is constant over a range interval, δx. Errors introduced by this assumption are negligible provided that δx is not too large.

The present implementation of equation (24) splits the field into even and odd parts after the inverse Fourier transform has been evaluated, applies a combination formula for these parts

which satisfies (26), then multiplies both parts by the environmental exponential term of (24) before reconstructing the full field from the even and odd parts, ready to begin solution at the next range step.

Losses due to irregular terrain and sea state conditions can also be incorporated into the model but these have not been addressed in this report.

4.2 Initial starting field

Since the tropospheric problem formulated in section 2.1 is an initial value one, it is necessary to specify the field at range x=0 in order to start the computational procedure. There are several ways that the starting field can be generated, the most obvious being to solve the full wave equation in a small region containing the source and to extend this out several wavelengths in range from the source to the region where the parabolic equation becomes valid (refer to restriction c, page 11). If the troposphere can be assumed to be exactly stratified near the source, then this solution can be obtained by separation of variables and calculation of the normal modes. This is, however, a rather complicated procedure considering that the energy of interest in ducting environments is merely that at small angles of incidence. Instead, the initial radiated field can be calculated with the aid of Fourier shifting theory.

From antenna theory, the radiated field is proportional to the Fourier transform of the field in the antenna aperture. Antenna pattern shape, height and steered direction can thus be modelled using the Fourier shift theorems to produce the starting field for calculations. This approach has been implemented in (Dockery, 1988) to specify arbitrary symmetric antenna patterns.

The approach taken by the author for examples included in section 7 is to model the starting field by a Gaussian function which is derived to assymptotically match the elliptic wave equation Green's function for a homogeneous atmosphere.

It is important to note that the initial field must be band-limited. The first reason for this arises because of the limit on propagation angle imposed by the parabolic approximation (refer to section 2.3.1 for details). There is however a further constraint imposed by the fast Fourier transform algorithm, as discussed in section 4.3.

4.3 Signal processing aspects

In order to assist examination of the signal processing aspects of the split step solution, it is useful to rewrite (24) in terms of dimensionless variables:

$$u(\tilde{x}+\delta\tilde{x},\tilde{z}) = \exp\{i\frac{\delta\tilde{x}}{2}[\tilde{n}_R^2(\tilde{x},\tilde{z}) + \tilde{n}_I^2(\tilde{x},\tilde{z})]\}\, f^{-1}[\exp\{\frac{-i\tilde{p}^2\,\delta\tilde{x}}{2}\}\, f(u)(\tilde{x},\tilde{p})] \qquad (29)$$

where

$$\tilde{z} = kz \qquad \tilde{p} = \frac{p}{k}$$

$$\tilde{x} = kx \qquad \delta\tilde{x} = k\,\delta x$$

are all measured in wavelengths; and $\tilde{n}_R^2(x,z)$, $\tilde{n}_I^2(x,z)$ are the real and imaginary components of the refractive index term that has been redefined in terms of wavelength.

The first issue of concern is the fact that the solution must satisfy the boundary condition that the field is attenuated to zero at infinite height. However, only a finite height can be accommodated by the discrete Fourier transform. In order to avoid unnecessarily large FFT sizes an absorbing layer is applied above the maximum altitude of interest to slowly attenuate the field, whilst at the same time minimising reflections from this interface.

The absorbing layer implemented in the examples included in section 7 was constructed by applying a simple raised cosine window to the imaginary part of the square of the refractive index term. From the first exponential term of (29) it is evident that this will cause an exponential attenuation. The raised cosine function was chosen for its differentiability, but other continuous functions can be applied for this purpose.

Another signal processing consideration is choice of FFT size. In order to avoid aliasing in the spatial frequency domain (p-space), sampling in height, z, should be no coarser than one half wavelength. For most applications, however, this would require very large transform lengths. Since only energy that is propagated at an angle near to horizontal will be trapped by ducting layers, it is reasonable to limit the maximum angle of propagation, Θ, that is to be considered by the solution. This restriction on Θ corresponds to a cut-off in the spatial frequency domain ($p = k \sin\Theta$) and so ignores that part of the spectrum which would otherwise contribute to aliasing. Sampling in the z-direction can now be coarser than the Nyquist half wavelength. For a specified maximum spatial frequency, p_{max}, the maximum height sample size, δz, which would avoid aliasing is given by $(2p_{max})^{-1}$ and the maximum altitude which can be considered is given (for a Fourier transform length of N) by $N\delta z/2$.

In the present implementation of the model, this low pass filtering of spatial frequency is achieved by applying a simple raised cosine window to the diffraction exponential term of (29) before the inverse Fourier transform is taken. This approach has been found by the author to be satisfactory for refractive structures implemented to date. More elaborate filtering may be found necessary, however, in other cases.

There is another non-trivial signal processing consideration. It is important to note that the value of p_{max} used to avoid aliasing in the spatial frequency domain should also take into account the allowable bound in the spatial domain, z. This is to ensure that aliasing does not result when either the forward or inverse transforms are taken after multiplication by the exponential terms of (29) in the spatial and spatial frequency domains. The required value of p_{max} will therefore be slightly less than that derived solely from N and δz as indicated in the previous paragraph.

5 SOLUTION PERTURBATION ANALYSIS

The purpose of this section is to examine the consequences of errors in estimating solution parameters. The effects of choice of range step size, δx, and height sample size, δz, have already been covered in sections 3.2 and 4.3 respectively. These however are parameters that can be chosen in order to give the desired accuracy (in the case of δx) or the maximum altitude/ angle of propagation that is to be considered by the solution (in the case of δz). What is investigated here is the effect that errors in the "measured" parameters have on solution. By "measured" is meant namely the refractive index, n, and initial field, u(0,z), components; these are the inputs to the system.

5.1 Perturbations in refractive index

Let the modified refractive index term of (24) be perturbed by a complex amount α and let the corresponding solution at range $x+\delta x$ be denoted by u'_{n-1}. Equation (24) can then be written for the perturbed and unperturbed cases as

$$u_{n+1} = e^{ikm'\delta x/2}\, \mathcal{F}^{-1}\{ e^{-ip^2 \delta x/2}\, \mathcal{F}(u_n) \}$$
$$u'_{n+1} = e^{ik(m'+\alpha)\delta x/2}\, \mathcal{F}^{-1}\{ e^{-ip^2 \delta x/2}\, \mathcal{F}(u'_n) \}$$

where $m' = m^2 - 1$. Then

$$u'_{n+1} - u_{n+1} = e^{ik(m'+\alpha)\delta x/2}\, \mathcal{F}^{-1}\{ e^{-ip^2 \delta x/2} [\mathcal{F}(u'_n) - \mathcal{F}(u_n)] \}$$
$$+ (e^{ik(m'+\alpha)\delta x/2} - e^{ikm'\delta x/2})\, \mathcal{F}^{-1}\{ e^{-ip^2 \delta x/2}\, \mathcal{F}(u_n) \}$$
$$= v_1 + v_2 \qquad (29)$$

where v_1, v_2 correspond to the terms of this sum. Now

$$|v_1| = e^{-k\{\mathrm{Im}(m'+\alpha)\}\delta x/2} \; | f^{-1}\{ e^{-ip^2 \delta x/2} [f(u'_n) - f(u_n)] \} |$$

where Im( ) denotes the imaginary part of ( ). So, finding the L_2 norm[2] of v_1 with respect to the measure $\frac{dp}{\sqrt{2\pi}}$,

$$||v_1|| \leq e^{-k\{\max_z\{\mathrm{Im}(m'+\alpha)\}\}\delta x/2} \; ||u'_n - u_n||$$

Similarly, the L_2 norm of v_2 is

$$\begin{aligned} ||v_2|| &\leq \max_z\{ |e^{ikm'\delta x/2}| \; |e^{ik\alpha\delta x/2} - 1| \} \; ||u_n|| \\ &\leq e^{-k\{\max_z(\mathrm{Im}(m'))\}\delta x/2} \quad \frac{k\delta x}{2} \; \max_z |\alpha| \; ||u_n|| \end{aligned}$$

Now, by applying the triangular inequality to (29),

$$\begin{aligned} ||u'_{n+1} - u_{n+1}|| &\leq ||v_1|| + ||v_2|| \\ &\leq e^{-k\{\max(\mathrm{Im}(m'+\alpha))\}\delta x/2} \; ||u'_n - u_n|| \\ &\quad + e^{-k\{\max(\mathrm{Im}(m'))\}\delta x/2} \; \frac{k\delta x}{2} \; \max_z |\alpha| \; ||u_n|| \end{aligned} \tag{30}$$

Let $\epsilon_n = ||u'_n - u_n||$, $\epsilon_{n+1} = ||u'_{n+1} - u_{n+1}||$. Then equation (30) is simply a difference equation of the form

$$\epsilon_{n+1} \leq A_n \epsilon_n + B_n$$

Recursively expanding this equation shows that

$$\epsilon_n \leq \Big(\prod_{j=1}^{n-1} A_j \Big) \epsilon_0 + \sum_{j=2}^{n} \Big\{ B_{n-j} \Big(\prod_{i=1}^{j-1} A_{n-i} \Big) \Big\} + B_{n-1}$$

Now

$$A_n \leq e^{-k\{\max(\mathrm{Im}(m'))\}\delta x/2} \; e^{-k\{\max(\mathrm{Im}(\alpha))\}\delta x/2} \leq 1$$

and

$$B_n = e^{-k\{\max(\mathrm{Im}(m'))\}\delta x/2} \; \frac{k\delta x}{2} \; \max_z |\alpha| \; ||u_n||$$

2. For discussion of the continuity properties of the Fourier Transform consult (Desoer and Vidyasagar, 1975).

Since $||u_n||$ is bounded, B_n will be bounded for all x,z. So for $A_n<1$, $\epsilon_n->0$, and for $A_n=1$, it is required that $\sum_n \max_z |\alpha(n\delta x,z)| < \infty$.

This implies that small perturbations in refractive index will tend to zero as the solution is stepped out in range and will not cause the solution to become unstable.

5.2 Perturbations in initial field

It is also important to consider perturbations in the initial field since these correspond to errors in calculation of the antenna field or to inaccuracies in the antenna pattern entered into calculations.

Rewriting equation (24)

$$u_{n+1} = e^{ik(m^2-1)\delta x/2} f^{-1}\{ e^{-ip^2 \delta x/2} [f(u_n)] \}$$
$$|u_{r+1}| = e^{-k[Im(m^2)]\delta x/2} | f^{-1}\{ e^{-ip^2 \delta x/2} [f(u_n)] \} |$$

The L_2 norm is then

$$||u_{n+1}|| \le \max_z e^{-k[Im(m^2)]\delta x/2} ||u_n||$$

Recursively expanding this equation shows that

$$||u_n|| \le \{ \prod_{j=0}^{n-1} \max_z e^{-k[Im(m^2)]\delta x/2} \} ||u_0||$$

and so

$$||u_n|| \le e^{knq\delta x/2} ||u_0||$$

where

$$q = \max_{x,z} Im\{m^2(x,z)\}$$

So the solution will be stable if $q \le 0$ and assymptotically stable if $q<0$. q will only be positive if energy is added to the system which is not the case for the dissipative nature of electromagnetic waves in the troposphere. Hence perturbations in the initial field will not result in instability.

6 REFRACTIVE VARIATIONS CAUSING DUCTING

Between 3 kHz and 3000 ghz the index of refraction is essentially independent of frequency. This index, n, is a value very close to unity and another index - radio refractivity, N - is commonly used for mathematical convenience:

$$N = (n - 1)\ 10^6$$
$$= 77.6\ P/T + 3.73 \times 10^5\ e/T^2 \qquad \text{(CCIR, 1986)}$$

where P = atmospheric pressure (mb)

T = absolute temperature (K)

e = water vapour pressure (mb)

In 'standard' atmospheric conditions each of these parameters (atmospheric pressure, temperature and water vapour pressure) decreases with increasing altitude. However, meteorological conditions often deviate from this standard atmosphere and an inversion layer of increasing refractivity with altitude may form. Radio refractivity gradient varies primarily due to variations in temperature and water vapour concentration, such variations occurring on time scales ranging from seconds to months. Values of these quantities are usually derived from radiosonde measurements, from which vertical profiles of refractive modulus, M, can be constructed. M is defined as

$$M = N + 10^6\ h/a$$

where h is height above the earth's surface and a denotes the earth's radius. Refractive modulus includes both atmospheric refraction and a correction term to account for the effects of the earth's curvature.

When the gradient of refractive modulus with respect to height is negative, ducting is present. Figures 4-6 contain three idealised refractive modulus profiles, each representing different categories of ducting. Figure 4(a) illustrates the presence of an evaporative duct, formed by an inversion layer at the surface of the earth. The duct extends from the earth surface to the top of the inversion layer, as indicated. This type of duct is regularly found over warm bodies of water and is generally caused by a temperature inversion near the surface that is accentuated by intense relative humidity as a result of evaporation. When this type of duct occurs over land it is usually referred to as a surface duct. As figure 4(b) illustrates, energy propagated from within the duct at a few degrees from horizontal will be trapped. Evaporation ducts are typically less than 10 m thick and surface values of refractive modulus around the world range between 300-400 M-units.

Figure 5(a) illustrates a profile in which an elevated duct is present. Such profiles contain two inflection points above the surface, each with a refractive modulus value greater than that at the surface. The duct, indicated on the profile by a vertical line, extends from the top of the inversion layer to the height at which the refractive modulus equals that at the upper duct boundary. As illustrated by figure 5(b), only energy launched into the duct at shallow angles will be trapped. Elevated ducts range in thickness from a few metres (these tend to affect propagation above microwave frequencies) up to hundreds of metres (affecting propagation at frequencies above VHF).

Figure 6(a) shows a surface-based elevated duct. The duct is elevated since two inflection points are present in the profile, but it is surface-based since the refractive modulus at the upper inflection point is less than that at the surface. Energy is trapped by the duct as indicated by the ray paths of figure 6(b).

The ray traces in figures 4-6 give an indication of the behaviour of energy in and around ducts, but do not indicate the relative strengths of that energy. Ducts which include both transmitter and receiver (target) will generally enhance the received signal, while the duct may act to shield the signal if transmitter or receiver (target) is situated outside the duct. Since refractive index commonly varies with range as well as with altitude, quite complex ducting structures are not uncommon, from which complicated field patterns emerge. What would be, at one specific altitude and range, an optimal location from which to communicate with a specified receiving point, could at a nearby position be quite shielded from the receiver. The advantage to be gained by a communications or surveillance system operator through a reliable propagation prediction technique is therefore obvious. The following examples of calculated field patterns for various ducting structures serve to illustrate the complicated nature of the effects on propagation that ducting can cause.

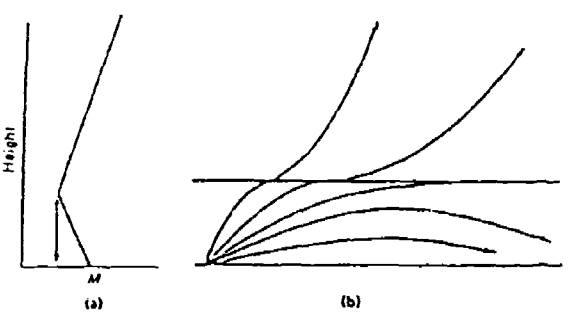

Figure 4 Ray paths and stylised vertical profile for evaporative duct

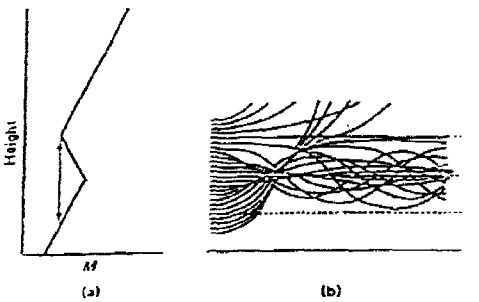

Figure 5 Ray paths and stylised vertical profile for elevated duct

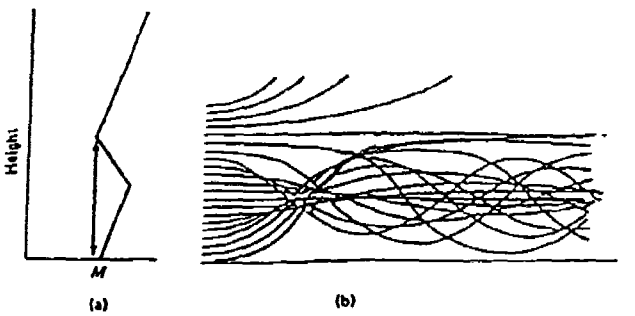

Figure 6 Ray paths and stylised vertical profile for surface-based elevated duct

7 COVERAGE DIAGRAM EXAMPLES

The split step Fourier solution to the parabolic wave equation has been implemented by the author on a personal computer with an in-board fast parallel processing card. The program is written in FORTRAN and uses a graphics display package called HGRAPH to produce coloured coverage diagrams of relative field strength on a height versus range flattened-earth grid. Execution times are directly proportional to the range out to which calculations are extended, and depend on the FFT sizes in the solution which are in turn dependent on frequency. As an indication, the examples in this section for the 1 ghz source took approximately two hours to generate for a range of 400 km (FFT size was 8192 points), while for the 100 MHz source, plots took approximately twenty minutes over

the same range (with FFT sizes of 1024 points). As indicated in section 4.3, the discretisation size in altitude (and therefore the length of the FFT) is related to the maximum allowable spatial frequency in p-space. This maximum spatial frequency directly relates to the maximum angle of propagation considered by the solution. So if energy at angles that are greater than this maximum is to be considered, then the altitude discretisation size will need to be decreased and therefore larger FFT sizes will be required. This will obviously increase execution times.

Note that, unlike for other full-wave methods, execution time is effectively independent of duct profile complexity. The qualifying "effectively" here is included because there may be cases in which the duct profiles need various amounts of interpolation to smooth discontinuities in the duct structures so as to reduce reflections from such irregularities. Such increases in execution time, however, will be independent of frequency and FFT lengths.

The examples included in section 7.1 all deal with range-independent ducting problems. That is, the ducting profiles used in these examples are horizontally homogeneous (they vary in height but not in range). These diagrams illustrate the effects on forward coverage that surface and elevated ducts cause. In section 7.2, these examples are extended to include problems that are range-dependent. Simple analytical structures are used to illustrate the complicated nature of the patterns resulting from such varying ducts.

7.1 Range-independent problems

Figure 7 represents the coverage of a 1 ghz vertically polarised Gaussian beam source at a height of 150 m in a "standard" exponential atmosphere (as defined by CCIR report 563-3, 1986). A perfectly conducting earth surface is assumed and the subsequent interference lobing is apparent. Figure 8 depicts this same source in a horizontally homogeneous elevated duct. The duct extends from approximately 50 m to 600 m and is of strength 55 M-units, as illustrated in the vertical refractive index profile beside the coverage diagram. The energy trapped by this duct is apparent. With reference to figure 8, it is clear that coverage is enhanced for heights below 600 m. Above this altitude, however, coverage is significantly reduced within 200 km from the source. At larger ranges, there is some leakage from the upper boundary of the duct. Note that unlike ray tracing techniques which tend to pass or reflect all of the energy at a duct interface, this parabolic approach permits partial energy reflection.

Another point which is important to note with reference to figure 8 is that, as a receiver (or target) moves through the duct, the received field varies as a function of height as well as of range. This is because of interference between waves which have undergone different

amounts of refraction/reflection, and also (to adopt ray tracing terminology) because of focusing effects. This point has been graphically illustrated in (Slingsby, 1990) where, for a horizontally homogeneous environment, radar signal returns are calculated using the modelling technique described in this report. The resulting plots of relative returned signal versus antenna height, and of relative returned signal versus target height, highlight the complicated effects that ducts have on signals and emphasise the need for an accurate prediction model. Thus, the knowledge that a duct is present is not sufficient to enable an operator to determine at which position a transmitter or receiver should be placed in order to optimise system performance.

In figure 9 the homogeneous ducting layer of figure 8 has been reduced in strength. The vertical refractive index profile for this diagram shows that this action has the effect of raising the base height of the duct and this is reflected in the coverage diagram. Because the duct is weaker, more energy escapes from the duct, as illustrated.

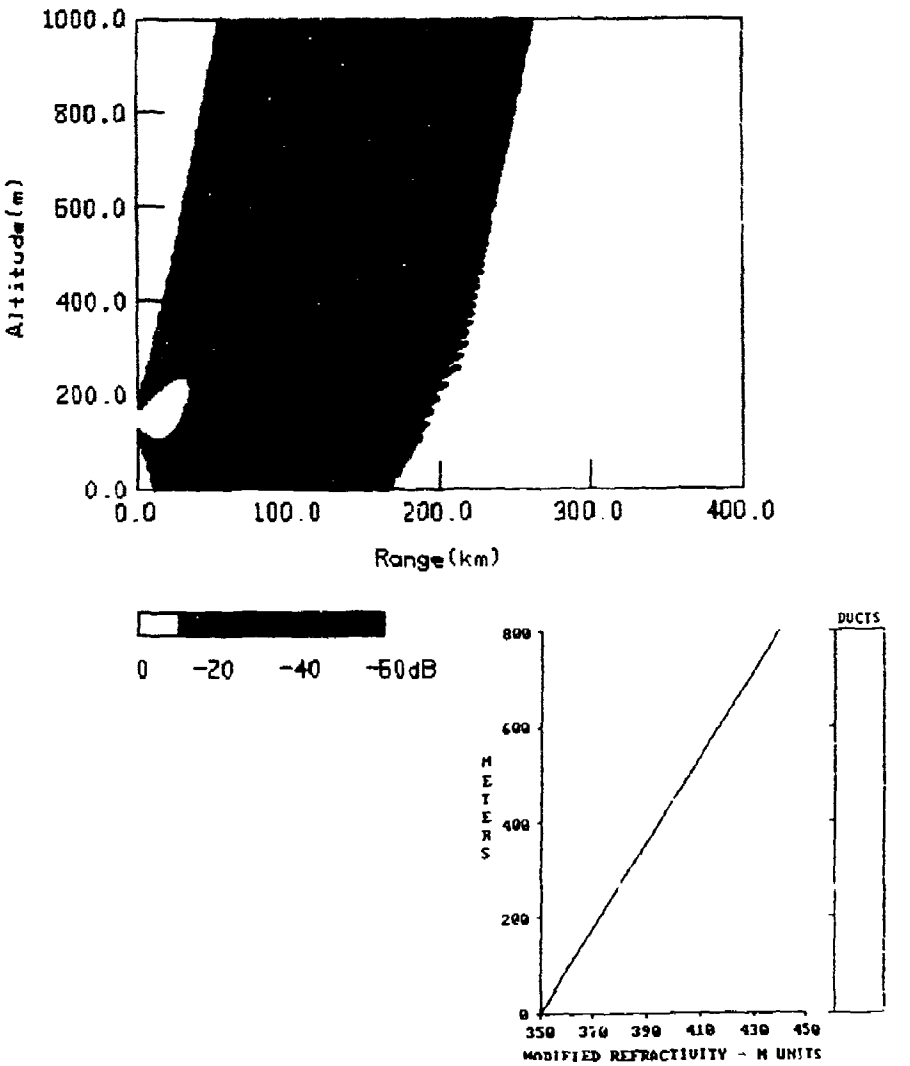

Figure 7 Coverage diagram for 1 GHz source in standard atmosphere

THIS PAGE INTENTIONALLY LEFT BLANK

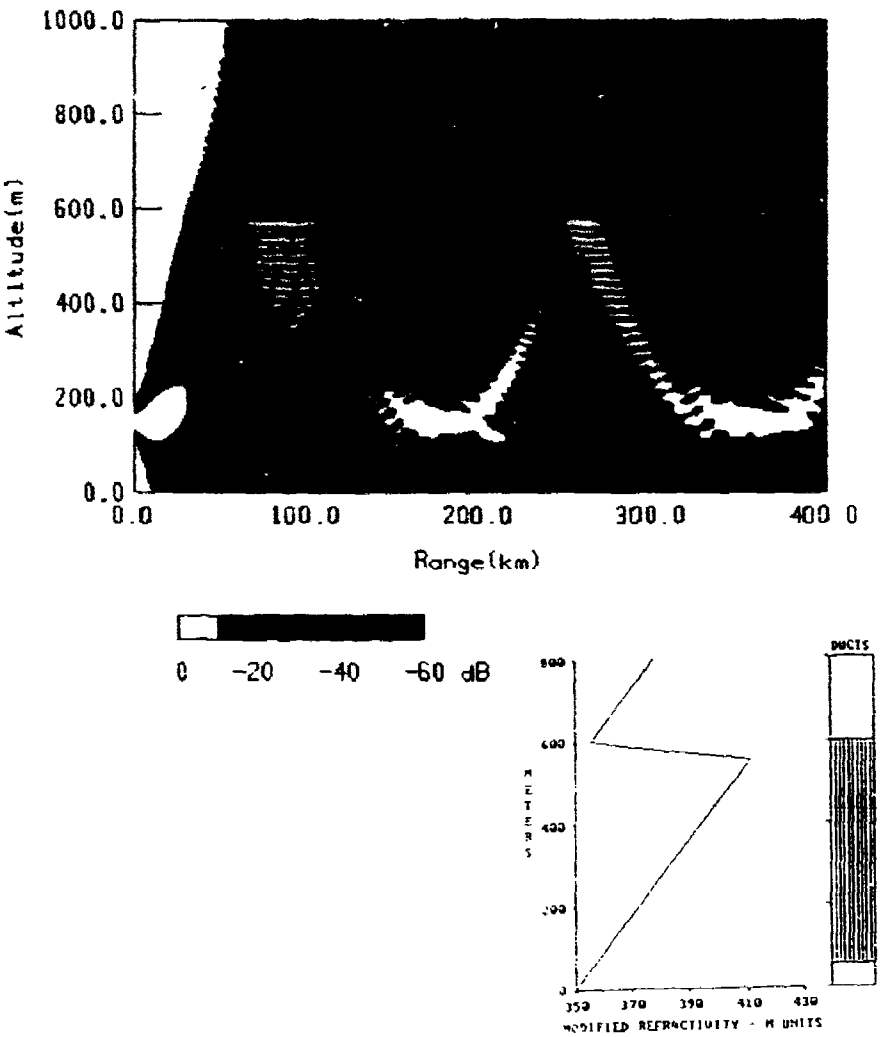

Figure 8 Coverage diagram for 1 GHz source in 55 M-unit homogeneous elevated duct

THIS PAGE INTENTIONALLY LEFT BLANK

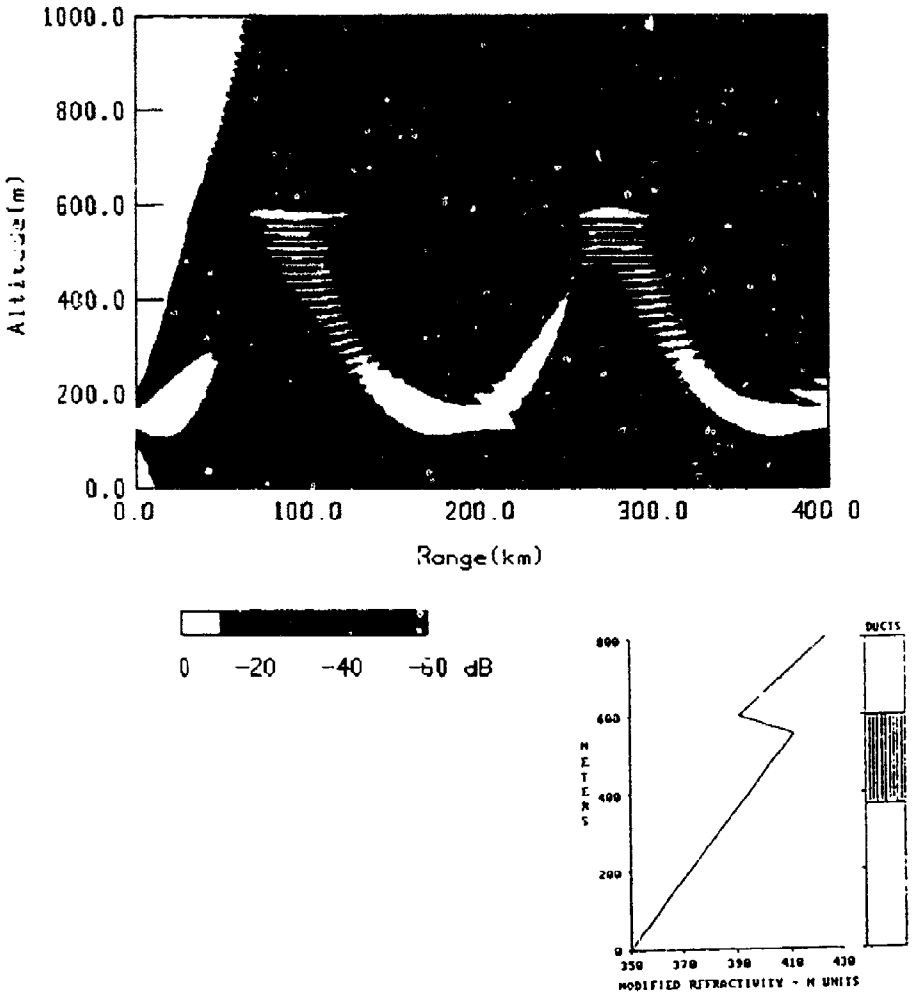

Figure 9 Coverage diagram for 1 GHz source in 20 M-unit homogeneous elevated duct

THIS PAGE INTENTIONALLY LEFT BLANK

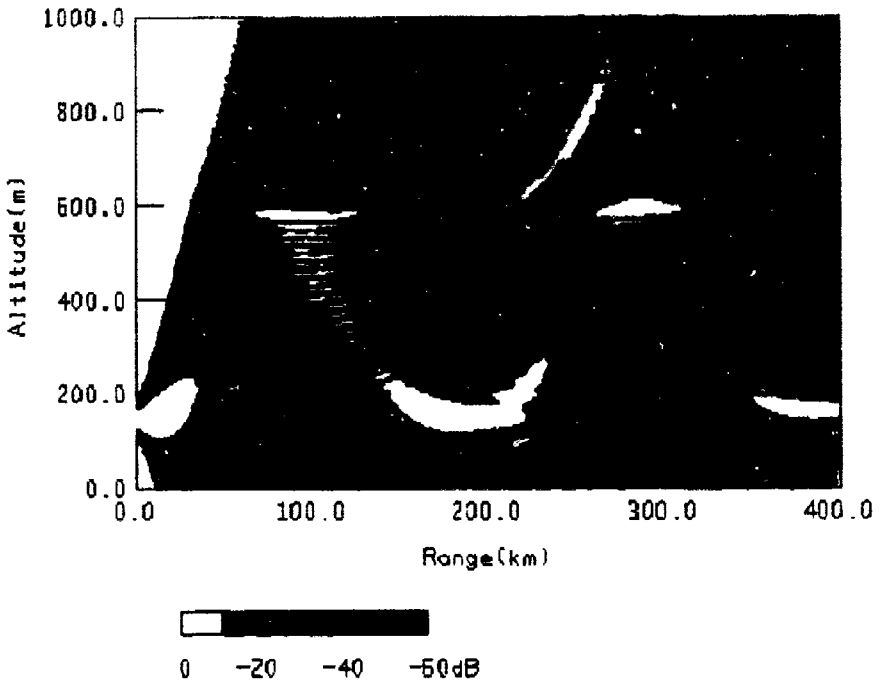

Figure 10 Coverage diagram for 1 GHz source in inhomogeneous duct

THIS PAGE INTENTIONALLY LEFT BLANK

7.2 Range-dependent problems

Figure 10 depicts the coverage for this same 1 GHz source, only this time in a non-homogeneous range-dependent environment. Study of this coverage diagram in light of the coverage diagram of figure 9, provides an indication of the inaccuracy incurred by assuming horizontal homogeneity. Both diagrams begin, at range x=0, with an elevated duct of 20 M-units at 600 m. Whilst the duct of figure 9 remains constant for all ranges, the duct of figure 10 has been weakened at a rate of 3 M-units per 100 km. Now this refractive modulus gradient is very slow; experimental results obtained for elevated ducts over the Timor Sea by (Barton, 1973), for example, indicate gradients of 32 M-units per 100 km. However the differences in coverage patterns are evident. With increasing range, much more energy begins to escape from the top of the duct of figure 10. As a result, the signal detected by a receiver placed 350km from the source at an altitude of 800 m, is 20 db stronger for the inhomogeneous ducting environment of figure 10 than for the case depicted in figure 9. But, on the other hand, a receiver 400 km from the source at an altitude of 630 km would detect a signal approximately 20 db weaker than would be predicted using the homogeneous ducting environment of figure 9.

The example given above highlights the fact that methods which use 'typical'[3] or 'interpolated'[4] vertical refractive index profiles to represent inhomogeneous ducting environments are susceptible to large errors in predicted signal coverage. The ability to model two-dimensionally inhomogeneous structures is clearly important. Making the assumption that a duct is horizontally uniform can cause significant underestimation of the level of leakage from the duct and can lead to field strength predictions that are substantially in error. Therefore, when elevated ducting structures are present, the most accurate model is the one prescribed in this report.

8 CONCLUSION

This report demonstrated the application of the parabolic equation method to range-independent and range-dependent tropospheric propagation modelling problems. The parabolic equation is an approximation to the Helmholtz wave equation which allows progressive calculation of the

3. This refers either to a vertical refractive index profile derived from measurements made at a single point along the propagation path or to a profile that is estimated by averaging profiles at several points along the path.

4. Commonly, a linear interpolation between vertical refractive index profiles is used to determine a representative profile for a particular range. Various authors perform what can appear to be something of a 'fudge' as they apply different methods of interpolation to these profiles in an attempt to verify experimental propagation results.

propagated electromagnetic field as solution is stepped out in range. The particular solution method described in this report and implemented at ERL derives from a technique developed by (Hardin and Tappert, 1973) for application to underwater acoustics problems. This 'split step Fourier' solution involves the discretisation of the field with respect to height and the use of the Fast Fourier transform at successive range points. The solution is stable, with errors being dependent on wavenumber, range step size and on the gradients of refractive index with respect to height and range. It has been shown in this report that the solution also behaves well for perturbations applied to the initial field and for small-scale discontinuities in refractive index profiles.

The propagation modelling method presented in this report has a number of advantages over other methods used to evaluate the effects of ducting layers on tropospheric propagation. The parabolic equation method retains all the diffraction effects associated with the propagating medium and therefore is valid in those regions where ray tracing techniques break down. Unlike ray tracing methods which give a qualitative picture of the effects of ducting on coverage, the method presented in this report uses a full-wave approach to calculate the amplitude function of the propagating signal. The method differs from coupled mode techniques in that it readily accommodates atmospheres which are horizontally inhomogeneous. Whereas for coupled mode techniques computational overhead is proportional to the intricacy of the duct profiles, computational intensity of the technique described in this report is independent of the duct profile complexity. By inviting a 'marching' solution the parabolic equation offers large computational saving over existing coupled mode techniques.

The examples given in section 7 of coverage diagrams generated with the parabolic equation technique serve to illustrate the complicated nature of the propagation patterns which arise due to ducting layers. It is particularly important to note the difference in coverage generated for a source in a horizontally inhomogeneous ducting atmosphere when compared with that same source in a homogeneous ducting atmosphere. Examples of this type highlight the realistic need for a mathematical model such as the one described in this report to accurately illustrate the effects that ducting layers have on propagation performance.

Whilst simple comparisons between the parabolic equation method and other existing techniques have been made by the author, verification against experimentally obtained propagation data has not yet been achieved. The reason for this is that very little experimental data is in existence. The atmospheric data necessary for the refractive index profiles that are input into the model is usually collected via radiosonde releases from the ground or via refractometer measurements from an aircraft. This can be a very expensive process and to date there exists very little data of this type that is concurrent with propagation measurements. This point raises the question of how much practical use such a mathematical model will have given present difficulties in attaining the input data. The

answer lies in the feasibility of remotely sensing this data by some other means than is currently employed. One possibility is the derivation of these profiles from meteorological satellite data. If this remote sensing can be achieved then the modelling technique described in this report will allow enhanced real-time evaluation of communications, surveillance or electronic warfare system performance.

REFERENCES

Barton, I. J. (1973). The importance of tilted layers in the tropospheric ducting of radio waves over the Timor Sea. *Radio Science*. Vol. 8, No 8. 727-32.

Booker, H. G. and Walkinshaw, W. (1946). The mode theory of tropospheric refraction and its relation to wave-guides and diffraction. *Conf. Proc. Meteorological Factors in Radiowave Propagation*. Phys. Soc. and Roy. Meteorol. Soc., London.

Budden, K. G. (1961). *The Wave-guide Mode Theory of Wave Propagation*. Prentice Hall, New Jersey.

CCIR. (1986). Radiometeorological Data. *Recommendations and Reports to the CCIR*. Vol. 5., Report 563-3.

Craig, K. H. (1985). Roots of the mode equation for propagation in an elevated duct. *Fourth International Conference on Antennas and Propagation (ICAP 85)*. 274-8.

Desoer, C.A., Vidyasagar, M. (1975). *Feedback Systems: Input-Output Properties*. Academic Press, New York.

Dockery, G.D. (1988). Modelling electromagnetic wave propagation in the troposphere using the parabolic equation. *IEEE Trans. Ant. Prop.* Vol. 36, No 10. 1464-70.

Fishback, W.T. (1951). Methods for calculating field strength with standard refraction. *Propagation of Short Radio Waves*. D.E. Kerr (ed.). McGraw-Hill. 112-40.

Hardin, R. H. and Tappert, F. D. (1973). Application of the split-step Fourier method to the numerical solution of nonlinear and variable coefficient wave equations. *SIAM*. Vol. 15. 423.

Hitney, H.V. and Richter, J.H. (1976). Integrated Refractive Effects Prediction System (IREPS). *Naval Engineer's Journal*, 88. 257-62.

Kerr, D. E. (ed.) (1951). *Propagation of Short Radio Waves*. McGraw-Hill.

Kewley, D. J., Sin Fai Lam, L. T. and Gartrell, G. (1984). Practical solutions of the parabolic equation model for underwater acoustic wave propagation. *Comp. Tech. Appl. (CTAC-83)*. 669-84.

Ko, H. W., Sari, J. W., Thomas, M. E., Herchenroeder, P. J. and Martone, P. J. (1984). Anomalous propagation and radar coverage through inhomogeneous atmospheres. *AGARD Conf. Proc.* 346. 25. 1-14.

Lee, D., Botseas, G. and Papadakis, J. (1981). Finite-difference solution to the parabolic wave equation. *J. Acoust. Soc. Am.* Vol. 70, No. 3. 795-800.

Lee, D. and Papadakis, J. (1980). Numerical solution of the wave parabolic equation: an ordinary-differential-equation approach. *J. Acoust. Soc. Am.* Vol. 68, No. 5. 1482-88.

Leontovich, M. A. and Fock. V. A. (1946). Solution of the problem of propagation of electromagnetic waves along the earth's surface by the method of parabolic equation. *J. Phys. USSR.* Vol. 10. No 1. 13-24.

Livingston, D.C. (1970). *The Physics of Microwave Propagation*. Prentice Hall, New Jersey.

Rotheram, S. (1983). Microwave duct propagation over the sea. *Third International Conference on Antennas and Propagation (ICAP 83)*. 9-13.

Senior, T. B. A. (1960). Impedance boundary conditions for imperfectly conducting surfaces. *Appl. Sci. Res.* Sec B. Vol. 8. 418-36.

Slingsby, P. L. (1990). Modelling of tropospheric propagation in ducting environments. *Proc. 1st Aust. Radar Conf. (RADARCON 90)*. Vol. 1, 119-25.

Steinberg, S. (1985). "Lie series, Lie transformations, and their applications" in Lie methods in optics. Mondragon, J.S. (ed.) *Lecture Notes in Physics*. 250. Springer-Verlag, Berlin, 56-64.

Wait, J. R. (1980). Coupled mode analysis for a nonuniform tropospheric wave guide. *Radio Science.* Vol. 15, No 3. 667-73.

DISTRIBUTION

	Copy No.
Defence Science and Technology Organisation	
Chief Defence Scientist) First Assistant Secretary, Science Policy (FASSP)) Assistant Secretary, Science Corporate Management)	1
Counsellor, Defence Science, London	Cont Sht Only
Counsellor, Defence Science, Washington	Cont Sht Only
Air Force Scientific Adviser	Cont Sht Only
Army Scientific Adviser	Cont Sht Only
Navy Scientific Adviser	Cont Sht Only
Electronics Research Laboratory	
Director, Electronics Research Laboratory	2
Chief, Communications Division	3
Chief, Electronic Warfare Division	4
Research Leader, Comms (CM)	5
Research Leader, Comms	6
Research Leader, Electronic Countermeasures	7
Research Leader, Signal & Inf Processing	8
Head, Radio Wave Propagation Group	9
Head, Communications Surveillance Systems	10
Head, Electronic Warfare Technology	11
Head, Electronic Countermeasures	12
Head, Electronic Support Measures Systems	13
Dr A. Kulessa, Electronic Support Measures Systems	14
Mr C. Wright, Radio Wave Propagation	15
Ms P. Slingsby, Radio Wave Propagation	16
Dr P. Baker, Radio Wave Propagation	17
Surveillance Research Laboratory	
Director, Surveillance Research Laboratory	18
Chief, Microwave Radar Division	19
Research Leader, Microwave Radar	20
Head, Microwave Radar Systems	21
Head, Electromagnetics	22
Head, Radar Techniques and Signal Processing	23
Head, Microwave Radar Engineering	24
Weapons Systems Research Laboratory	
Director, Weapons Systems Research Laboratory	25
Research Leader, Guided Weapons Division	26
Head, Combat System Effectiveness	27
Head, Operations Research	28
Head, Exercise Analysis	29

Libraries and Information Services

Librarian, Technical Reports Centre, Defence Central Library, Cambell Park	30
Document Exchange Centre, Defence Information Services	31
Joint Intelligence Organisation (DSTI)	32
Defence Science and Technology Organisation, Main Library	33-34
Librarian Defence Signals Directorate Melbourne	35
Library ARL	36
National Library of Australia	37
Library Department of Transport and Communications	38
Australian Defence Force Academy Library	39
United States Defense Technical Information Center	40-41
United Kingdom Defence Research Information Centre	42-43
Director Scientific Information Services, Canada	44
New Zealand Ministry of Defence	45
British Library Document Supply Centre	46
Spares	47-53

Department of Defence

DOCUMENT CONTROL DATA SHEET

Page Classification
UNCLASSIFIED
Privacy Marking/Caveat
-

1a. AR Number	1b. Establishment Number	2. Document Date	3. Task Number
AR-006-452	ERL-0531-RR	SEPT 90	-

4. Title

TROPOSPHERIC PROPAGATION MODELLING WITH THE PARABOLIC EQUATION

5. Security Classification

Document	Title	Abstract
U	U	U

S (Secret) C (Confi) R (Rest) U (Unclass)

* For UNCLASSIFIED docs with a secondary distribution LIMITATION, use (L)

6. No. of Pages	44
7. No. of Refs.	22

8. Author(s)

Patricia L. Slingsby

9. Downgrading/Delimiting Instructions

-

10a. Corporate Author and Address

Electronics Research Laboratory
PO Box 1600
SALISBURY SA 5108

10b. Task Sponsor

-

11. Officer/Position responsible for

Security ..... -

Downgrading ..... -

Approval for Release ..... DERL

12. Secondary Release of this Document

APPROVED FOR PUBLIC RELEASE

Any enquiries outside stated limitations should be referred through DSTIC, Defence Information Services, Department of Defence, Anzac Park West, Canberra, ACT 2600.

13a. Deliberate Announcement

No Limitations

13b. Casual Announcement (for citation in other documents)

[X] No Limitation

[ ] Ref. by Author & Doc No only

14. DEFTEST Descriptors

Tropospheric Propagation
Parabolic Differential Equations
Helmholtz Equation

15. DISCAT Subject Codes

0401

16. Abstract

The parabolic equation is a full-wave approximation to the Helmholtz wave equation that, unlike existing ray tracing and coupled mode techniques, readily accommodates two-dimensionally inhomogeneous atmospheres. This report discusses implementation of a split-step Fourier Transform solution to the parabolic equation and includes examples of coverage diagrams calculated by this method.

Page Classification
UNCLASSIFIED
Privacy Marking/Caveat

16. Abstract (CONT.)

17. Imprint

Electronics Research Laboratory
PO Box 1600
SALISBURY SA 5108

18. Document Series and Number	19. Cost Code	20. Type of Report and Period Covered
RESEARCH REPORT 0531	603542	–

21. Computer Programs Used

None

22. Establishment File Reference(s)

None

23. Additional information (if required)